CHEMICAL ENGINEERING TRANSACTIONS
VOL. 111, 2024
A publication of AIDIC
The Italian Association of Chemical Engineering
Online at www.cetjournal.it
Guest Editors: Valerio Cozzani, Bruno Fabiano, Genserik Reniers

ISBN 979-12-81206-11-3; **ISSN** 2283-9216
DOI: 10.3303/CET24111076

Modelling Fire Response of Cryogenic Liquid Hydrogen Tanks Equipped with Multilayer Insulation (MLI) Systems

Davide Camplese[a,*], Giordano Emrys Scarponi[a], Robert Eberwein[b], Aliasghar Hajharir[b], Frank Otremba[b], Valerio Cozzani[a]

[a]Alma Mater Studiorum - Università di Bologna, Dipartimento di Ingegneria Civile, Chimica, Ambientale e dei Materiali, via Terracini 28, 40131 Bologna, Italy
[b]Bundesanstalt für Materialforschung und -prüfung (BAM), Berlin
davide.camplese@unibo.it

In the context of the growing global interest in hydrogen-based green energy, cryogenic tanks equipped with multi-layer insulation (MLI) are emerging as a leading solution for storing hydrogen in vehicles. The integrity of these systems might be threatened during fire exposure. This can trigger the degradation of the MLI materials and induce rapid pressurization of the tank with a high risk of catastrophic failure. In this work, a novel lumped model to simulate the thermal response of MLI-equipped cryogenic liquid hydrogen tanks is presented. The model integrates the accurate database "Coolprop" for hydrogen thermodynamic properties and sub-models for detailed simulation of MLI degradation, providing a realistic simulation of the experimental data obtained under normal operating conditions. The application of the model to several case studies considering different numbers of MLI layers and tank geometries demonstrates that aluminum-based MLI offers scarce protection in case of exposure to a hydrocarbon poolfire.

1. Introduction

Moving toward more sustainable energy sources, hydrogen has emerged as a highly promising alternative to traditional fuels due to its reduced environmental footprint (Preuster et al., 2017). The storage of hydrogen as a liquid (LH_2) within cryogenic tanks equipped with multilayer insulation (MLI) stands out as an effective solution for hydrogen-powered vehicles, ensuring high volumetric energy density (Kunze and Kircher, 2012). MLI systems consist of multiple layers of low-emissivity material, radiative layers, interleaved with high-free volume spacers. These are housed within the double-walled shell of the vessel, operating in high-vacuum conditions. MLI minimizes heat leakage into the vessel with a thinner thickness if compared to other insulation materials (Edward and Filip, 2018).
Besides the advantages associated with the widespread deployment of LH_2 new technologies, there are also significant hazards to consider due to the high flammability of hydrogen. An accidental loss of integrity of these types of vessels could result in extremely dangerous phenomena, such as BLEVEs (Boiling Liquid Expanding Vapor Explosion) and fireballs (van Wingerden et al., 2022). This situation may occur as a consequence of exposure to external heat sources, such as fires triggered by road accidents. Despite the super-insulating properties of MLI, the results of fire exposure tests suggest that these materials may undergo severe degradation at high temperatures (Eberwein et al., 2023), leaving the tank almost unprotected from the fire heat flux and leading to failure in a relatively short time (Pehr, 1996).
In this framework, the availability of models able to simulate cryogenic hydrogen tank response is crucial to ensure a safe design and support emergency response planning. Recently, several CFD and lumped models were developed for this purpose. For instance, Scarponi et al. (2016) proposed a lumped approach to simulate the pressure build-up and temperature behavior of liquefied natural gas (LNG) tanks under fire attack. Ustolin et al. (2022) successfully implemented a CFD simulation of an MLI-equipped LH_2 tank engulfed in fire. In both models, good agreements with experimental data were only possible by setting the insulation equivalent thermal conductivity to higher values than those measured at normal operating conditions. However, the instant of time

Paper Received: 25 February 2024; Revised: 10 April 2024; Accepted: 6 July 2024
Please cite this article as: Camplese D., Scarponi G.E., Eberwein R., Hajharir A., Otremba F., Cozzani V., 2024, Modelling Fire Response of Cryogenic Liquid Hydrogen Tanks Equipped with Multilayer Insulation (MLI) Systems, Chemical Engineering Transactions, 111, 451-456 DOI:10.3303/CET24111076

at which the value of thermal conductivity shall be augmented was empirically determined for the specific case. Therefore, this approach can not be extended to different MLIs, tank geometries, and fire scenarios.
The present study introduces a novel lumped model to simulate the pressure build-up of MLI-insulated cryogenic LH_2 tanks in fire scenarios considering the MLI degradation at high temperatures to overcome existing limitations. The model integrates the accurate database “Coolprop” (Bell et al., 2014) for hydrogen thermodynamic properties and the sub-model proposed by Camplese et al. (2023) for detailed simulation of aluminum-based MLI degradation. The effectiveness of the model in simulating the pressurization of such tanks is demonstrated in non-fire conditions by comparison with experimental results. Then, several case studies were defined to assess the impact of MLI characteristics and tank geometry on the pressurization time under hydrocarbon poolfire exposure. The results provide valuable information to support the safe design of MLI-equipped LH_2 cryogenic tanks and emergency management in case of fire accidents.

2. Methodology

The methodology proposed to predict the pressurization of cryogenic LH_2 tanks engulfed in fires was divided into two stages. The first one (Section 2.1) is devoted to the model definition. The second one (Section 2.2) describes the experimental test used as a reference to assess the model reliability. Section 2.3 defines the case studies considered to assess the tank response under fire conditions applying the developed model.

2.1 Model description

The lumped model proposed for the determination of the pressurization rate of MLI-equipped cryogenic liquefied hydrogen tanks engulfed in fire is based on a thermal nodes approach. The tank domain is divided into N+2 nodes as shown in Figure 1: one node for the fluid domain, *F*, one for the tank external shell, S_e, and one for each radiative layer of the MLI, *1* to *N*. A transient thermal heat balance is written for each node and reported in Table 1 together with the other model equations.
The heat balance for the tank lading is solved with Eq(1) by assuming thermodynamic equilibrium between liquid and gaseous hydrogen phases (they share the same temperature, T_F). This single-zone approach avoids both the definition and quantification of the heat transfer mechanisms at the liquid-vapor interface, for which a reliable correlation is still lacking in the literature. The focus of the study is to predict the pressurization rate before the activation of any pressure relief system. Therefore, the tank system is considered closed to mass exchanges and the total mass balance is not solved. Once the internal energy of the system is obtained from the heat balance, the “Coolprop” database (Bell et al., 2014) is used at each timestep to estimate the physical properties of the liquid and gaseous hydrogen phases and then the system pressure.
The novelty of the present model lies in the accurate representation of the heat transfer through the MLI both in normal operating and in fire-induced degradation conditions. In Eq(1), A_S represents the inner shell surface and q_S is the heat flux to the inner tank. The last one is computed as the heat flux coming from the innermost MLI layer (i.e., node *1*) or from the external shell surface (i.e., node S_e) if the MLI is completely degraded. If the characteristic dimension of the vessel significantly exceeds the gap between the two vessel shells and homogeneous fire boundary conditions are present on the tank surface, the heat transfer occurs only in the direction normal to the surface of the MLI layer, resulting in a one-dimensional approach. Eq.s(2) to (4) express the thermal balances for all the N nodes of the MLI. The heat flux from the i-th radiative layer to the (i-1)-th is a modified version of the McIntosh (1994) classical "layer by layer" model to account for vacuum loss cases.

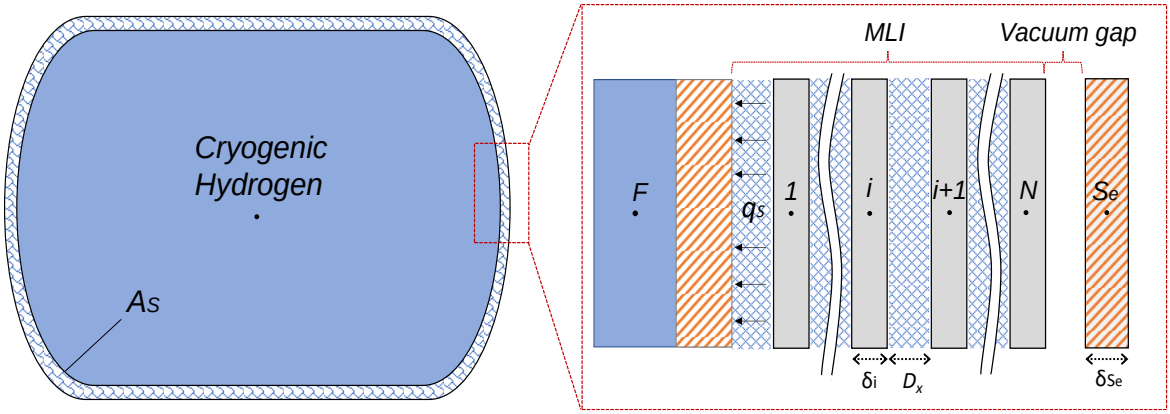

Figure 1. Schematic representation of the thermal node discretization. L = liquid, Se = external shell, rl = radiative layer. Nodes 1 to N refer to the MLI radiative layers.

Table 1. Set of the equation used in the MLI-equipped cryogenic LH_2 tank model.

Node	Variable	Equation	Eq. N°
F	U_F	$\frac{dU_F}{dt} = q_S A_S$	(1)
1	T_1	$\delta_{rl}\rho_{rl}c_{p\_rl}\frac{dT_1}{dt} = q_{rl,2} - q_{rl,1}$	(2)
i	T_i	$\delta_{rl}\rho_{rl}c_{p\_rl}\frac{dT_i}{dt} = q_{rl,i+1} - q_{rl,i}$	(3)
N	T_N	$\delta_{rl}\rho_{rl}c_{p\_rl}\frac{dT_N}{dt} = \frac{1}{\left(\frac{1}{\varepsilon_{S_e}}+\frac{1}{\varepsilon_N}-1\right)}\sigma\left(T_{S_e}^4 - T_N^4\right) + q_{g,Se} - q_{rl,N}$	(4)
Se	T_{Se}	$\delta_{S_e}\rho_{S_e}c_{p\_S_e}\frac{dT_{S_e}}{dt} = \varepsilon_{S_e}\sigma\left(T_{BB\_fire}^4 - T_{S_e}^4\right) - \frac{1}{\left(\frac{1}{\varepsilon_{S_e}}+\frac{1}{\varepsilon_N}-1\right)}\sigma\left(T_{S_e}^4 - T_N^4\right) - q_{g,Se}$	(5)
-	$q_{rl,i}$	$q_{rl,i} = q_{rad,i} + q_{s,cond,i} + q_{g,i}$	(6)
-	$q_{rad,i}$	$q_{rad,i} = \frac{\sigma}{\left(\frac{1}{\varepsilon_i}+\frac{1}{\varepsilon_{i-1}}-1\right)}\left(T_i^4 - T_{i-1}^4\right)$	(7)
-	$q_{s,cond,i}$	$q_{s,cond,i} = \frac{C_2 f k_s}{D_x}(T_i - T_{i-1})$	(8)
-	$q_{g,i}$	$q_{g,i} = \begin{cases} q_{g,cond,i} & if\ Gr < 2860 \\ q_{g,conv,i} & if\ Gr \geq 2860 \end{cases}$	(9)
-	$q_{g,cond,i}$	$q_{g,cond,i} = \left[\frac{D_x}{k_g} + \frac{2-\theta}{\theta}\cdot\frac{\sqrt{\frac{\pi MT}{2R}}}{\left(1+\frac{\zeta}{4}\right)P_r}\right]^{-1}(T_i - T_{i-1})$	(10)
-	$q_{conv,i}$	$q_{g,conv,i} = Nu\frac{k_g}{D_x}(T_i - T_{i-1})$	(11)

This is calculated as the sum of three different heat transfer mechanisms ($q_{,rl}$, Eq(6)). The first one is the thermal radiation between each layer ($q_{,rad}$, Eq(7)). The second one is the solid conduction through the spacer material ($q_{s,cond}$, Eq(8)). The last mechanism is the heat transfer through gas (q_g, Eq(9)). This is represented by gas conduction ($q_{g,cond}$, Eq(10)), expressed according to Sherman (1963), when the Grashof number, *Gr,* is lower than 2860 (Xie et al., 2010). Otherwise, gas convection prevails ($q_{g,conv}$, Eq(11)), which is calculated according to Xie et al. (2010). All the N nodes share the same heat balance, except for the 1-st and the N-th ones. In fact, these face the inner and outer shells, respectively. Since the 1-st radiative layer is separated from the inner shell of the vessel by a single spacer, the thermal balance in node 1 preserves the same form as those shown for the other layers, but Eq(2) has to be modified considering the emissivity of the inner shell surface material. On the contrary, a vacuum gap is present between the outer shell and the N-th radiative layer. Therefore, solid spacer conduction does not contribute to the overall heat flux entering the N-th node, $q_{rl,N}$, in Eq(4). The high-temperature degradation of the MLI is simulated by assuming that each radiation layer is completely and instantaneously destroyed once its temperature reaches a specific degradation temperature, T_{deg}. Then, the layer is replaced by a vacuum gap of the same thickness and only radiation, convection, and gas conduction are considered to exist between the first undamaged layer and the external shell. Further details on the degradation model are presented elsewhere (Camplese et al. 2023). Finally, Eq(5) is used to solve the heat balance on the external shell node, S_e, where the heat transfer from the fire is simulated by assuming that the external wall is uniformly exposed to thermal radiation from a constant black body temperature (T_{BB_fire}).

2.2 Comparison with experimental results

Detailed experimental data on MLI-equipped LH_2 tanks exposed to fire are still lacking in the literature. For this reason, the model effectiveness in predicting the pressure build-up of such tanks was tested against the experimental results on a liquid nitrogen (LN_2) tank in case of loss of vacuum within the MLI system (Xie et al., 2012). It is worth mentioning that this condition causes severe deterioration of the insulation performance and should be taken under consideration when dealing with the safety aspects of LH_2 tanks.

The LN_2 tank geometries and the MLI system characteristics of the case under investigation are listed elsewhere (Xie et al. 2012). The 50 % of the tank volume was initially filled with liquid nitrogen at atmospheric pressure in equilibrium with its vapor. At the starting point of the test, the insulation system was abruptly filled with gaseous nitrogen up to atmospheric pressure. Then, the pressure build-up inside the tank was measured.

2.3 Case studies

The modeling approach presented in Sections 2.1 and 2.2 was applied to a set of case studies to assess the impact of the volume of the tank and the MLI configurations on pressure build-up during fire exposure scenarios. Three different horizontal tank geometries, representative of the most commonly adopted sizes in storage tanks used for cryogenic hydrogen-powered vehicles, were considered by fixing a length-to-diameter (L/D) ratio equal to 2. These are reported in Table 3**,** where A_s was calculated by assuming the tank as a cylinder with a length equal to L and a diameter equal to D.

Table 2. Tank geometries considered in the case studies.

Case study	L (m)	D (m)	V (m^3)	A_s (m^2)
CASE A	1	0.5	0.2	2
CASE B	1.7	0.85	1	5.8
CASE C	2.5	1.25	3	12

In each case, 50% of the tank was filled with liquid hydrogen at ambient pressure and saturation conditions. The external shell material was AISI 304, while AISI 316L was chosen for the internal shell. The thicknesses were 0.003 m and 0.002 m, respectively. The tanks featured a typical commercial uniform-density MLI composed of pure aluminum radiative layers and glass fiber fleece spacers. The vacuum gap had a thickness of 0.03 m and the residual gas inside was air. All the other data needed to close the model set of equations for the specific MLI considered are listed in Table 3.

Table 3. MLI geometrical and material properties.

Property	Symbol	Unit	Radiative layer	Spacer
Material	-	-	Aluminum	Glass fiber fleece
Thickness	δ_{rl}/D_x	m	$6 \cdot 10^{-6}$	$2.44 \cdot 10^{-4}$
Density	ρ	kg/m^3	2700	2500*
Thermal Conductivity	k	W/(m·K)	250	0.8*
Heat capacity	c_p	J/(kg·K)	900	-
Relative density	f	-	-	0.01
Emissivity	ε	-	0.04	-
Spacer empirical factor	C_2	-	-	0.0025
Residual gas pressure	P_r	Pa	$1 \cdot 10^{-3}$	
Layers number	N	-	20 - 80	20 - 80
*solid material properties				

Each simulation run shared the same MLI parameters, except for the number of layers (N). This was varied between 20 and 80, covering the most common commercial applications. According to previous works (Camplese et al., 2023), the degradation temperature (T_{deg}) was set to 660 °C, which is the melting point temperature of the aluminum. A full engulfing hydrocarbon pool fire was selected as fire scenario, defined according to the guidelines proposed by Birk Albrecht et al. (2016): the T_{BB_fire} was set to 871 °C. A timestep of 0.1 s was selected for all cases. The initial temperature profile in each node corresponds to the steady-state solution obtained considering constant boundary temperatures: a liquid temperature of -252.75 °C and an outer shell temperature of 20 °C. This is representative of the system condition prior to fire exposure.

3. Results and discussion

Figure 2a reports the results of the comparison between experimental and modeling data of the self-pressurization of the LN_2 tank undergoing loss of vacuum within the insulation system (see Section 2.2), which consists of an aluminum-based MLI with 30 layers. A good prediction of the experimental data was obtained for the studied case. The simulated pressure values have an average relative error of 7 %, which results in a slightly conservative prediction of the total time of pressurization (i.e., 288 min of the model against 300 min of the experimental measurement). Figure 2b compares the experimental temperature distribution over time within the MLI with the modeling results for the case in which the tank lading is kept at atmospheric conditions after the loss of vacuum scenario (Xie et al., 2010). The maximum difference between measured and simulated temperatures comes from the 30th layer and stands at 10 K. This result demonstrates that the heat flux on the inner shell is well predicted by the model. Overall, the simulation results agree with the experimental data.

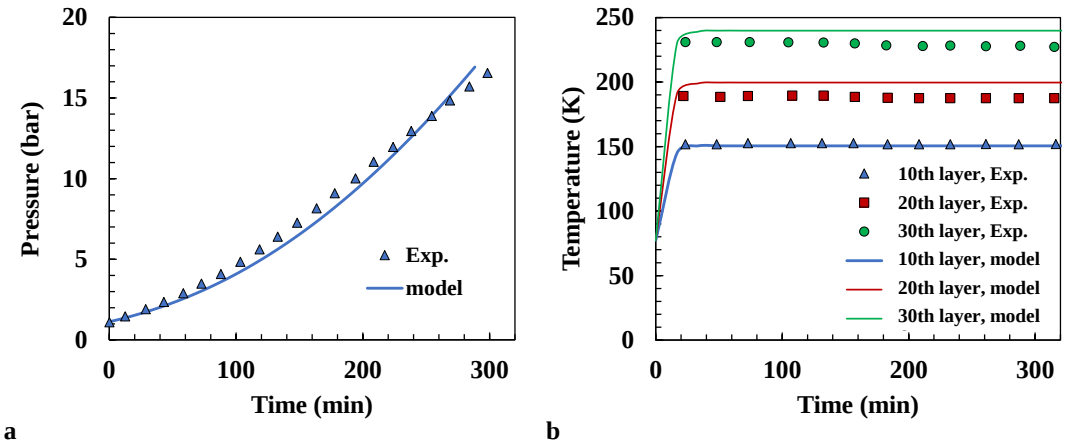

Figure 2. Modeling (continuous lines) versus experimental (points) results: (a) pressurization curves for a LN_2 tank with MLI (30 layers) under loss of vacuum conditions; (b) temperature distribution within the MLI after nitrogen gas leaking in the insulation jacket. Experimental data from (Xie et al., 2012) and (Xie et al., 2010).

Figure 3 shows the impact of the number of MLI layers, N, on the activation time (t_{PRV}) of the pressure relief valve (PRV) (set to 4.7 bar as in the fire test conducted by Pehr (1996)) for the three case studies. In all the case studies, the MLI is completely degraded before t_{PRV}. The dynamics of insulation degradation and its effect on the heat flux entering the tank are presented in previous works (Camplese et al., 2023), and hence not discussed here. The t_{PRV} varies within a span of 4 min, ranging from 3.7 min in the worst-case scenario (i.e., CASE A with 20 layers) to 7.7 minutes in the best-case one (CASE C with 80 layers). These results are in line with experimental observations by Pehr (1996). Overall, the outcomes demonstrate scarce performances of aluminum-based MLI systems in case of fire exposure. However, tanks equipped with MLIs with a high number of layers are prone to delayed pressurization. A linear correlation was found between t_{PRV} and N (see Figure 3). On the contrary, the tank volume has no significant effects on t_{PRV} for the specific geometry considered. In fact, by increasing the tank volume by a factor of 15, the maximum difference in t_{PRV} stands at 0.5 min.

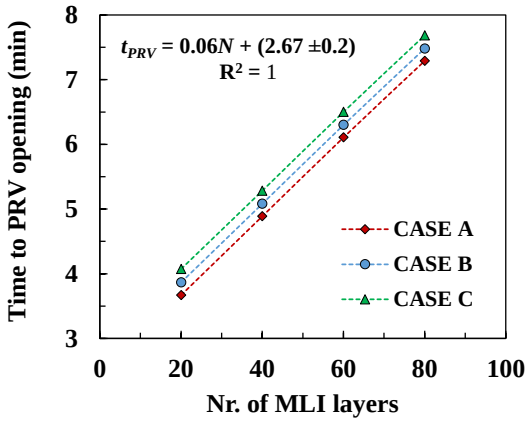

Figure 3. PRV activation time versus the number of MLI layers for LH_2 tanks engulfed in a hydrocarbon poolfire.

4. Conclusions

The problem of predicting the thermal response of MLI-equipped cryogenic liquid hydrogen tanks exposed to fire was addressed by developing an equilibrium model that integrates the accurate simulation of aluminum-based MLI performance deterioration at high temperatures. The model performed well in predicting both the pressurization and the heat flux toward the tank when compared to experimental data concerning normal operating conditions. The results obtained from the application to realistic case studies demonstrate that MLI protection under poolfire conditions is limited to a few minutes, highlighting a significant challenge in ensuring tank integrity during fire accidents. The best performances came out from MLIs with a higher number of layers. On the contrary, the pressure build-up was not influenced by the tank volume for a fixed length-to-diameter ratio. These insights are valuable for enhancing emergency response strategies and devising mitigation measures to ensure the integrity of cryogenic tanks.

Acknowledgments

This work is part of the NICOLHy project (No. 101137629) funded by the EU and Clean Hydrogen Partnership. Views and opinions expressed are however those of the authors only and do not necessarily reflect those of the EU or Clean Hydrogen JU. Neither the EU nor the granting authority can be held responsible for them.

Nomenclature

T = temperature, K
q = heat flux, W/m^2
P = pressure, Pa
P_r = residual gas pressure within the spacer, Pa
N = number of radiative layers, -
c_p = specific heat capacity at constant pressure, J/(kg·K)
R = universal gas constant, J/(mol·K)
ρ = density, kg/m^3
δ = thickness, m
A_s = surface area of the inner shell, m^2
L = length of the inner vessel, m
D = diameter of the inner vessel, m
V = tank volume, m^3
M = molecular weight, kg/mol
γ = specific heat ratio, -
σ = Stefan-Boltzmann coefficient, W/(m^2·K^4)
θ = accommodation factor (0.88 for Nitrogen), -
ζ = gas molecular degree of freedom (2 for Nitrogen), -
C_2 = empirical constant for the spacer material, -
f = relative density of the spacer to the solid material, -
D_x = thickness of the spacer, m
k_s = thermal conductivity of the solid spacer material, W/(m·K)
k_g = residual gas thermal conductivity, W/(m·K)
ε = emissivity of the material surface, -
m = mass, kg
Nu = Nusselt number, -
t_{PRV} = time to pressurization up to PRV opening, min
Gr = Grashof number, -

References

Bell, I.H., Wronski, J., Quoilin, S., Lemort, V., 2014. Pure and Pseudo-pure Fluid Thermophysical Property Evaluation and the Open-Source Thermophysical Property Library CoolProp. Ind. \& Eng. Chem. Res. 53, 2498–2508.

Birk Albrecht, M., Otremba, F., Gonzalez, F., Prabhakaran, A., Borch, J., Bradley, I., Bisby, L., 2016. Fire Testing of Total Containment Pressure Vessels. Chem. Eng. Trans. 48, 277–282.

Camplese, D., Chianese, C., Scarponi, G.E., Eberwein, R., Otremba, F., Cozzani, V., 2023. Analysis of High Temperature Degradation of Multi-layer Insulation (MLI) Systems for Liquid Hydrogen Storage Tanks. Chem. Eng. Trans. 99, 415-420.

Eberwein, R., Hajhariri, A., Camplese, D., Emrys Scarponi, G., Cozzani, V., Otremba, F., 2023. Insulation Materials Used in Tanks for the Storage of Cryogenic Fluids in Fire Scenarios, in: Volume 6: Operations, Applications, & Components. American Society of Mechanical Engineers.

Edward, L., Filip, L., 2018. Influence of vacuum level on insulation thermal performance for LNG cryogenic road tankers, in: MATEC Web of Conferences. EDP Sciences, p. 1019.

Kunze, K., Kircher, O., 2012. Cryo-compressed hydrogen storage cryogenic cluster day. Oxford, Sept. 28, 2012.

McIntosh, G.E., 1994. Layer by Layer MLI Calculation Using a Separated Mode Equation, in: Kittel, P. (Ed.), Advances in Cryogenic Engineering. Springer US, Boston, MA, pp. 1683–1690.

Pehr, K., 1996. Experimental Examinations on the Worst Case Behavior of LH2/LNG Tanks for Passenger Cars, in: Proceedings of the 11th World Hydrogen Energy Conference, Stuttgart, Germany. pp. 2169–2186.

Preuster, P., Alekseev, A., Wasserscheid, P., 2017. Hydrogen Storage Technologies for Future Energy Systems. Annu. Rev. Chem. Biomol. Eng. 8, 445–471.

Scarponi, G.E., Landucci, G., Ovidi, F., Cozzani, V., 2016. Lumped model for the assessment of the thermal and mechanical response of LNG tanks exposed to fire. Chem. Eng. Trans. 53, 307–312.

Sherman, F.S., 1963. A survey of experimental results and methods for the transition regime of rarefied gas dynamics. Rarefied Gas Dyn. Vol. 2 2, 228.

Ustolin, F., Scarponi, G.E., Iannaccone, T., Cozzani, V., Paltrinieri, N., 2022. Cryogenic Hydrogen Storage Tanks Exposed to Fires: a CFD Study. Chem. Eng. Trans. 90, 535–540.

van Wingerden K., Kluge M., Habib A. K., Ustolin F., Paltrinieri N., 2022, Medium-scale Tests to Investigate the Possibility and Effects of BLEVEs of Storage Vessels Containing Liquified Hydrogen. Chemical Engineering Transactions, 90, 547–552.

Xie, G.F., Li, X.D., Wang, R.S., 2012. Experimental study on the storage performance of high-vacuum-multilayer- insulation tank after sudden, catastrophic loss of insulating vacuum. Heat Mass Transf. und Stoffuebertragung 48, 757–766.

Xie, G.F., Li, X.D., Wang, R.S., 2010. Study on the heat transfer of high-vacuum-multilayer-insulation tank after sudden, catastrophic loss of insulating vacuum. Cryogenics (Guildf). 50, 682–687.